J Fluoresc (2009) 19:285–289
DOI 10.1007/s10895-008-0414-2

ORIGINAL PAPER

$Gd_2(MoO_4)_3:Er^{3+}$ Nanophosphors for an Enhancement of Silicon Solar-Cell Near-Infrared Response

X. F. Liang · X. Y. Huang · Q. Y. Zhang

Received: 22 April 2008 / Accepted: 11 August 2008 / Published online: 21 August 2008

Abstract In an attempt to take full advantage of near-infrared part of the solar spectrum, $Gd_2(MoO_4)_3:Er^{3+}$ nanophosphors have been proposed as potential luminescent materials to enhance the response of the silicon solar-cell. Upon excitation with low-energy near-infrared photons, intense upconverted emissions at 545, 665, 800, and 980 nm, for which energies higher than the bandgap of silicon solar-cell, have been achieved with conversion efficiencies of 0.12%, 0.05%, 0.83%, and 1.35%, respectively. Development of nanophosphors for photovoltaic purposes could open up an approach in achieving high-efficiency silicon-based solar-cell by means of the up-conversion of the sub-bandgap near-infrared part of the solar spectrum (E<1.12 eV) to visible/near-infrared photons.

Keywords Upconversion · Nanophosphors · Rare-earth ions · Solar cells

Introduction

The standard air-mass (AM1.5) terrestrial spectrum covers the wavelength region from UV to IR (200–2500 nm). However, silicon solar-cell could only absorb UV-Vis-IR radiation with energies larger than that of the band gap of 1.12 eV which corresponds to wavelengths shorter than 1,100 nm. One possibility to reduce the transmission losses of the sub-band-gap radiation is by up-conversion of the transmitted low-energy near-infrared (NIR) photons from the solar spectrum to high-energy photons upon the exploring the upconversion (UC) mechanism [1–11], which can then be utilized by the silicon solar-cell. Recently, Gibart et al. [1] have demonstrated the feasibility of this concept experimentally by stacking a rare-earth (RE) doped vitroceramic behind a substrate-free GaAs solar-cell. Trupke et al. [2] have determined theoretically that the upper limit of the photovoltaic conversion efficiency of a single junction solar-cell coupled to an UC ideal device as 47.6%, when the sun has been modeled as a 6,000 K blackbody and 50.7% under AM1.5 terrestrial spectrum, and Shalav et al. [3] have reported a $NaYF_4:Er^{3+}$ upconverting phosphor and shown a maximum external quantum efficiency (QE) of silicon solar-cell of 2.5% with the doping concentrations of Er^{3+} as high as 20%. However, the external QE of 2.7% in $NaYF_4:xEr^{3+}$ (x=20% molar) seems on the lower side by taking the concentration quenching (CQ) into account when the doping concentrations of Er^{3+} beyond 20%, which strongly reduces the luminescence yield. Moreover, fluoride may not be a suitable phosphor matrix because of its undesirable chemical nature.

Here in the present paper, our main objective is to make an attempt to make full utilization of NIR part of the solar spectrum, to meet this purpose, $Gd_2(MoO_4)_3:Er^{3+}$ ($GM:Er^{3+}$) nanophosphors have been proposed as potential luminescent materials to enhance silicon solar-cell NIR response. Er^{3+} is considered to be suitable for photovoltaic UC purposes since the spectral power from the normalized 1,000 W/m^2 AM1.5 spectrum yields over 100 W/m^2 between 1,100 and 1,700 nm, which match well with the energy gap of the $^4I_{15/2}\rightarrow{}^4I_{13/2}$ transition (~1,500 nm) of Er^{3+} [3–5]. Structural and luminescent properties of $GM:Er^{3+}$ nanophosphors have been investigated here. Our results show that intense UC emissions at 545, 665, 800, and 980 nm with energies greater than the band gap of silicon solar-cell have been achieved upon excitation with NIR photons provided by a tunable laser (1510–1565 nm), the conversion efficiencies are 0.12%, 0.05%, 0.83%, and 1.35%, respectively. Our investigation reveals that

X. F. Liang · X. Y. Huang · Q. Y. Zhang (✉)
Key Lab of Specially Functional Materials of Ministry of Education and Institute of Optical Communication Materials, South China University of Technology, Guangzhou 510641, People's Republic of China
e-mail: qyzhang@scut.edu.cn

in principle it is an efficient luminescent converter, which in an ideal case, converts NIR photons into visible/NIR photons by exploiting UC mechanism. By taking into account the thermal stability and the high efficiency of the matrix, the GM:Er^{3+} nanophosphors could be identified as potential materials for applications in high efficiency silicon-based solar-cell and nano-photonics.

Experimental details

Synthesis of GM:Er^{3+} nanophosphors

Powder samples of $Gd_{2-x}(MoO_4)_3$:xEr^{3+} (x=0.05, 0.1, 0.2, 0.3 and 0.5) (in molar) nanophosphors were prepared by means of combustion synthesis, as described in Refs. [12–14]. In brief, Gd_2O_3 (99.99%), Er_2O_3 (99.99%), $(NH_4)_6Mo_7O_{24}{\cdot}4H_2O$ (A.R.), nitric acid and citric acid were used as raw materials. Gd_2O_3 and Er_2O_3 were firstly dissolved in HNO_3 to form RE nitrates solutions. Then, to prepare the mixture solution of ammonium molybdate and organic components, $(NH_4)_6Mo_7O_{24}{\cdot}4H_2O$ and citric acid were dissolved in mixture solvent of ethylene glycol (A.R.) and distilled water. Finally, the previously prepared RE nitrates solutions were added dropwise to the mixed solution of ammonium molybdate and organic components with a molar ratio of $(2-x)Gd^{3+}$:xEr^{3+}:3 $[MoO_4]^{2-}$(x=0.05, 0.1, 0.2, 0.3 and 0.5), the mixture was then heated in an induction heating plate with temperature range from 100–250°C for 10 min with vigorous stirring. The obtained amorphous solid precursors were then pulverized carefully in corundum crucibles, and calcined at the temperature of 950 °C for 10 h.

Characterization

The products were analyzed by means of X-ray diffraction (XRD, Philips Model PW1830, CuKα), micro-Raman spectrometer (Renishaw model RM 2000), scanning electron microscopy (SEM, JEM-1010), transmission electron microscopy (TEM, JEOL 2010), and fluorescence spectrometer (Jobin-Yvon TRIAX320 equipped with a Hamamatsu R928 and R5108 photomultiplier tube. A Santec TSL-210 tunable laser (1510–1565 nm), a Coherent 808 nm laser diode (LD), and the 488 nm line of a Coherent Sabre Innova Ar^+ laser were used as the excitation sources).

Results and discussion

Structural characterization

Shown in Fig. 1(a) are the XRD pattern and Raman spectrum of the obtained $Gd_{2-x}(MoO_4)_3$:xEr^{3+} (x=0.1) nanocrystals. The XRD pattern agrees well with the standard diffraction (JCPDS card no. 20-0408), revealing a single-phase orthorhombic GM with the lattice parameters of a=10.388, b=10.416 nm, c=10.697 nm, and has a space group of Pba2 (32). The stronger diffraction peaks appear at 25.5°, 29.4° and 26.9°, correspond to the (221), (222), and (022) planes respectively. In gadolinium molybdate compounds, intense Raman bands are found from 750 to 1,000 cm^{-1} and 250 to 400 cm^{-1} at room temperature. The strong band near 900 cm^{-1} in the Raman spectrum of GM is assigned to the υ_1 symmetric stretching mode of Mo–O [15], the band near 840 cm^{-1} is assigned to υ_3 antisymmetric vibration of Mo–O, while the bands located at the region of 250–400 cm^{-1} are assigned to υ_2(E) and υ_4(T_2) bending modes of MoO_4^{2-} ions [15]. Raman spectrum confirms that a single phase GM is formed in our samples. It is noted that codoping limited Er^{3+} with respect to Gd^{3+} ions does not cause any significant change in the host structure, which is due to the similarity of the ion radii and also due to existence of the equal electric charges between Gd^{3+} and dopants Er^{3+}. The typical SEM image of the nanocrystals is shown in the inset of Fig. 1b. It can be seen that the nanocrystals show homogeneous size with narrow size distribution and mean sizes in the range from 80–120 nm in diameter, which is larger than the calculated data from Debye-Scherre's equation indicating that these particles are composed of nanosized polycrystalline. A typical TEM image shown in Fig. 1c indicates the uniform GM:Er^{3+} nanocrystals with smooth surface. The corresponding selected area diffraction pattern is shown in the inset of Fig. 1c.

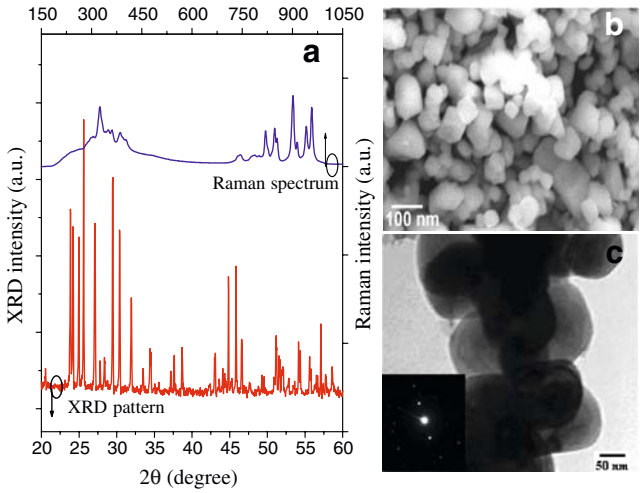

Fig. 1 **a** XRD pattern and Raman spectrum of GM:Er^{3+} nanocrystals. **b** a typical SEM image of the nanocrystals. **c** TEM image of the GM:Er^{3+} nanocrystals, *inset* shows the corresponding selected area electron diffraction pattern

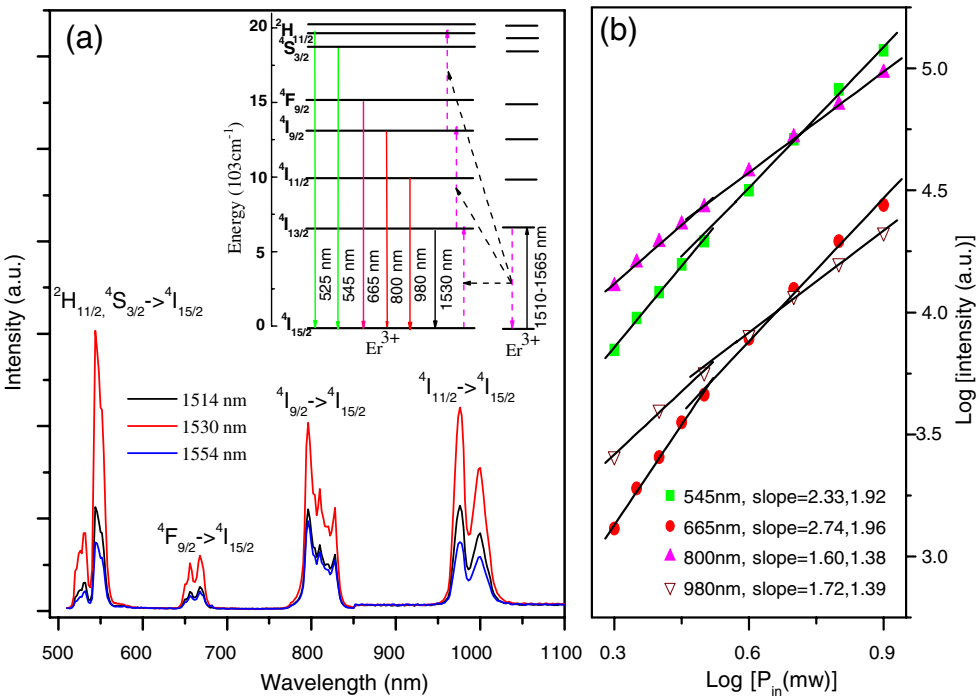

Fig. 2 **a** Visible-NIR UC emission spectra of GM:Er^{3+} nanophosphors upon excitation with tunable laser. *Inset* shows schematic energy levels of the nanophosphors showing possible mechanisms for UC process under excitation of visible with tunable laser. **b** Log–log plot of the UC intensity versus the pumping power

Spectral properties

Figure 2 presents the upconverted emission spectra of GM:Er^{3+} anophosphors upon excitation with a tunable laser. The intense green emissions at 530 and 545 nm are assigned to Er^{3+} $^2H_{11/2}\rightarrow{}^4I_{15/2}$ and $^4S_{3/2}\rightarrow{}^4I_{15/2}$ transitions, respectively, while the red one at 665 nm is ascribed to Er^{3+} $^4F_{9/2}\rightarrow{}^4I_{15/2}$ transition. Two intense NIR emissions at 800 and 980 nm have also clearly been observed and are assigned to Er^{3+} $^4I_{9/2}\rightarrow{}^4I_{15/2}$, and $^4I_{11/2}\rightarrow{}^4I_{15/2}$ transitions, respectively. The dependence of the UC intensity (I_{UC}) upon the excitation power (P) was investigated and the results are presented in log-log plot in the right side of Fig. 2. Remarkably, the data could be divided into two groups for all the four transitions following to the relationship of $I_{UC} \propto P^n$, where n is the pumping photons required to excite RE ions from ground state to the emitting excited state. At low power levels (P≤0.5 mW, 500 W/m^2), the results revealed cubic power law behaviors for the 545 and 665 nm visible emission signals and quadratic power law behaviors for the 800 and 980 nm NIR signals with the slopes of the linear fittings are 2.33 for $^4S_{3/2}\rightarrow{}^4I_{15/2}$, 2.74 for $^4F_{9/2}\rightarrow{}^4I_{15/2}$, 1.60 for $^4I_{9/2}\rightarrow{}^4I_{15/2}$, and 1.72 for $^4I_{11/2}\rightarrow{}^4I_{15/2}$, respectively. However, for higher excitation power levels, the saturation of the energy UC process takes place and the corresponding slopes of the linear fittings drop down to 1.92, 1.96, 1.38, and 1.39 respectively, attributing to the competition between the linear decay and the UC processes for the depletion of the intermediate excited states [16]. The possible energy transfer between Er^{3+}, as well as the proposed mechanisms to explain the UC luminescence in GM:Er^{3+} nanophosphors are demonstrated in detail in the inset of the figure (Fig. 2, left).

The dependence of the aforementioned four UC emission transitions on the incident laser wavelengths in the range of 1,510–1,565 nm are shown in the Fig. 3. Obviously, for all the four transitions, intense broadband emissions have been observed with at excitation at 1530 nm. The inset figure of Fig. 3 illustrates the dependence of the UC intensity upon

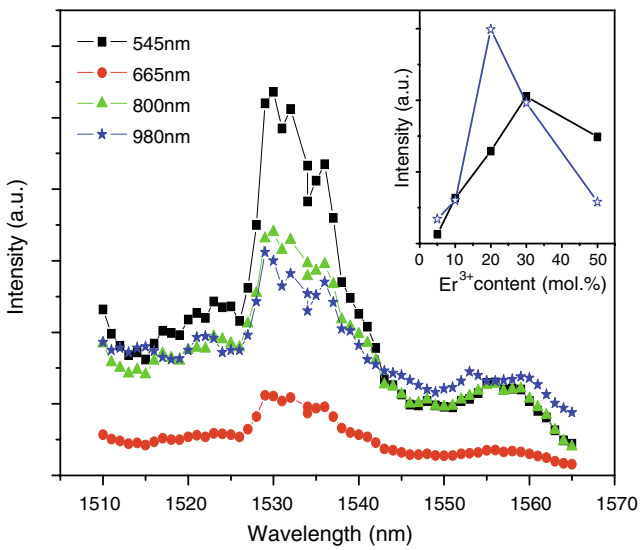

Fig. 3 The dependence of the four UC emission transitions on the incident laser wavelengths in the range of 1,510–1,565 nm. *Inset* shows the dependence of the green- and NIR-emission intensity on the Er^{3+} doping-concentration in GM:Er^{3+} nanophosphors

the Er^{3+} doping-concentration of GM nanophosphors under excitation of 1,530 nm. It is noticed that the UC intensity of the green-emission at 545 nm increases rapidly with an increase of Er^{3+} concentrations ranging from 1 to 30 mol%. However, a decrease has clearly been observed when Er^{3+} concentration is set to be more than 30 mol%, due to the CQ. While, for the NIR-emission at 980 nm, maximum emission has been obtained upon optimizing the Er^{3+} concentration as 20 mol%.

The GM:Er^{3+} nanophosphors yields a predominantly green upconversion emission [($^2H_{11/2}$,$^4S_{3/2}$)→$^4I_{15/2}$] in the spectrum excited by 1,510–1,565 nm radiation, as shown in Fig. 2. The upconversion efficiency for this transition could be determined by comparing the upconversion luminescence signal with the directly excited signal intensity, which is given by [17, 18]:

$$\eta = \eta_q \left(\frac{P_{\mathrm{abs}}(\mathrm{Vis})}{P_{\mathrm{abs}}(\mathrm{NIR})} \right) \left(\frac{I_{\mathrm{emit}}(\mathrm{upconverted})}{I_{\mathrm{emit}}(\mathrm{direct})} \right) \quad (1)$$

where P_{abs}(Vis) is the absorbed light power for direct excitation with 488 nm laser or 808 nm LD, and P_{abs}(NIR) is the absorbed light power for upconversion excitation with 1,510–1,565 nm tunable laser, which were determined from the measured incident light power, the absorption coefficient and the absorption path length in the sample. The luminescence intensities I_{emit}(upconverted) and I_{emit}(direct) are the recorded portion of the emitted light at 545 nm measured under the same light collecting conditions. The quantum efficiency η_q for direct excitation is defined as [17, 18]:

$$\eta_q = \frac{\tau_{\mathrm{exp}}}{\tau_R} \quad (2)$$

where τ_{exp} is the measured lifetime with excitation of 488 nm, and τ_{R} is the radiative lifetime obtained from the Judd–Ofelt theory [19, 20]. τ_{exp} of the $^4S_{3/2}$, $^4F_{9/2}$, and $^4I_{9/2}$ states of GM:Er^{3+} were determined to be 0.126, 0.068, and 0.824 ms, respectively. For the NIR emission at 980 nm [$^4I_{11/2}$→$^4I_{15/2}$], the measured lifetime, τ_{exp}, was obtained upon excitation with 808 nm LD and was found to be 0.915 ms. The radiative lifetime (τ_{R}) of the $^4S_{3/2}$, $^4F_{9/2}$, $^4I_{9/2}$ and $^4I_{11/2}$ states of Er^{3+} in GM:Er^{3+} nanophosphors were estimated to be 0.299, 0.364, 3.412 and 3.199 ms according to the previous reports [21]. The incident light power density employed in this study has been found to be 1.8, 20, and 0.5 W/cm^2 for the 488 nm line of the Ar^+ laser, 808 nm LD, and the NIR tunable laser, respectively. The obtained upconversion efficiencies for the NIR to green-emission at 545 nm, red-emission at 665 nm, and NIR emissions at 800 and 980 nm were 0.12%, 0.05%, 0.83%, and 1.35%, respectively. The relatively high η in the GM:Er^{3+} nanophosphors might be due to the high Er^{3+} content, the low phonon energy, and the high refractive index of the nanophosphors.

Conclusion

In summary, we briefly conclude that intense upconverted four emissions at 545, 665, 800, and 980 nm with energies greater than the bandgap of silicon solar-cell have been measured from GM:Er^{3+} nanophosphors upon excitation with low-energy NIR photons provided by a tuable laser ranging 1,510–1,565 nm. The obtained upconversion efficiencies for the four upconverted emissions were 0.12%, 0.05%, 0.83%, and 1.35%, respectively. The development of GM:Er^{3+} nanophosphors as upconverted luminescent materials could open up a potential possibility in realizing a high efficiency silicon-based solar-cell by upconverted the sub-bandgap NIR part of the solar spectrum (E<1.12 eV) to visible/NIR photons.

Acknowledgments The authors would like to acknowledge financial support from NSFC (Grant No.50602017) and DSTG (Grant No.2006J1-C0491).

References

1. Gibart P, Auzel F, Guillaume JC, Zahraman K (1996) Below band-gap IR response of substrate-free GaAs solar cells using two-photon up-conversion. Jpn J Appl Phys 35(Part 1):4401–4403. doi:10.1143/JJAP.35.4401
2. Trupke T, Green MA, Wurfel P (2002) Improving solar cell efficiencies by up-conversion of sub-band-gap light. J Appl Phys 92:4117–4122. doi:10.1063/1.1505677
3. Shalav A, Richards BS, Trupke T, Kramer KW, Gudel H (2005) Application of $NaYF_4$:Er^{3+} up-converting phosphors for enhanced near-infrared silicon solar cell response. Appl Phys Lett 86:013505. doi:10.1063/1.1844592
4. Bird RE, Riordan C (1986) Simple solar spectral model for direct and diffuse irradiance on horizontal and tilted planes at the earths surface for cloudless atmospheres. J Clim Appl Meteorol 25:87–97. doi:10.1175/1520-0450(1986)025<0087:SSSMFD>2.0.CO;2
5. Richards BS (2006) Luminescent layers for enhanced silicon solar cell performance: Downconversion. Sol Energy Mater Sol Cells 90:1189–1207. doi:10.1016/j.solmat.2005.07.001
6. Digonnet MJF (2001) Rare-earth-doped fiber lasers and amplifiers. Marcel Dekker, New York
7. Reisfeld R, Jorgensen CK (1977) Lasers and excitated states of rare-earth. Springer, Berlin
8. Ryba-Romanowski W, Golab S, Dominiak-Dzik G, Slarz P, Lukasmer T (2001) Conversion of infrared radiation into red emission in YVO_4:Yb,Ho. Appl Phys Lett 79:3026–3028. doi:10.1063/1.1415767
9. Hehlen MP, Kramer K, Gudel HU, McFarlane RA, Schwarts RN (1994) Up-conversion in Er^{3+} -dimer systems-trends within the series $Cs_3Er_2X_9$ (X=Cl,Br,I). Phys Rev B 49:12475–12484. doi:10.1103/PhysRevB.49.12475
10. Zhang QY, Li T, Jiang ZH, Ji XH, Buddhudu S (2005) 980 nm laser-diode-excited intense blue upconversion in Tm3+ /Yb3+ -codoped gallate-bismuth-lead glasses. Appl Phys Lett 87:171911. doi:10.1063/1.2115082
11. Zhang QY, Yang CH, Pan YX (2007) Cooperative quantum cutting in one-dimensional $Yb_xGd_{1-x}Al_3(BO_3)_4$: Tb3+ nanorods. Appl Phys Lett 90:021107. doi:10.1063/1.2430942

12. Pan YX, Zhang QY, Jiang ZH (2007) Comparative Investigation on Nanocrystal Structure and Luminescence Properties of Gadolinium Molybdates Codoped with Er^{3+}/Yb^{3+}. J Fluoresc 17:444–451. doi:10.1007/s10895-007-0191-3
13. Yang CH, Pan YX, Zhang QY (2007) Cooperative energy transfer and frequency upconversion in Yb^{3+}–Tb^{3+} and Nd^{3+}–Yb^{3+}–Tb^{3+} codoped $GdAl_3(BO_3)_4$ phosphors. J Fluoresc 17:500–504. doi:10.1007/s10895-007-0200-6
14. Pan YX, Zhang QY, Zhao C, Jiang ZH (2007) Luminescent properties of novel Ho^{3+} and Tm^{3+} doped gadolinium molybdate nanocrystals synthesized by the Pechini method. Solid State Commun 142:24–27. doi:10.1016/j.ssc.2007.01.029
15. Lucazeau G, Machon D (2006) Polarized Raman spectra of $Gd_2(MoO_4)_3$ in its orthorhombic structure. J Raman Spectro 37:189–201. doi:10.1002/jrs.1456
16. Pollnau M, Gamelin DR, Lüthi SR, Güdel HU, Hehlen MP (2000) Power dependence of upconversion luminescence in lanthanide and transition-metal-ion systems. Phys Rev B 61:3337–3346. doi:10.1103/PhysRevB.61.3337
17. Pan ZD, Morgan SH, Dyer K, Ueda A (1996) Host-dependent optical transitions of Er^{3+} ions in lead-germanate and lead-tellurium-germanate glasses. J Appl Phys 79:8906–8913
18. Vetrone F, Boyer JC, Capobianco JA, Speghini A, Bettinelli M (2002) 980 nm excited upconversion in an Er-doped ZnO-TeO_2 glass. Appl Phys Lett 80:1752–1754. doi:10.1063/1.1458073
19. Judd BR (1962) Optical absorption intensities of rare-earth ions. Phys Rev B 127:750–761
20. Ofelt GS (1962) Intensities of crystal spectra and decay of Er^{3+} fluorescence in LaF_3. J Chem Phys 37:511–520. doi:10.1063/1.1701366
21. Qian Q, Wang Y, Zhang QY, Yang GF, Jiang ZH (2008) Spectroscopic properties of Er^{3+}-doped Na_2O-Sb_2O_3-B_2O_3-SiO_2 glasses. J Non-Cryst Solids 354:1981–1985. doi:10.1016/j.jnoncrysol.2007.11.005